

Investigations of TiO₂ Photocatalysts for the Decomposition of NO in the Flow System

The Role of Pretreatment and Reaction Conditions in the Photocatalytic Efficiency

Jinlong Zhang,¹ Terukazu Ayusawa, Madoka Minagawa, Kensaku Kinugawa, Hiromi Yamashita, Masaya Matsuoka, and Masakazu Anpo²

Department of Applied Chemistry, Osaka Prefecture University, 1-1 Gakuen-cho, Sakai, Osaka 599-8531, Japan

Received August 24, 1999; revised March 14, 2000; accepted September 18, 2000; published online February 7, 2001

In order to investigate the photocatalytic stability and/or lifetime of titanium oxide photocatalysts in detail, standard reference photocatalysts (JRC-TiO-2, -3, -4, and -5), of which the surface chemical and physical properties are well known, were studied for the photocatalytic decomposition of NO under a large-scale flow reaction system. In the first stage, the photocatalytic decomposition of NO proceeded with a high efficiency and continuous production of N₂, O₂, and N₂O. However, the reaction efficiency gradually decreased and finally leveled off at constant values. These values were found to be in the order of JRC-TiO-4 > -3 > -5 > -2. Anatase TiO₂, with a large surface area and numerous OH groups, was found to exhibit a high efficiency for the decomposition of NO in the flow system. The optimal pretreatment and reaction conditions were observed at a pretreatment temperature around 573 K under a mixture of O₂ and Ar. It was confirmed that the surface hydroxyl groups on the photocatalysts play an important role in the decomposition of NO under this flow system. © 2001 Academic Press

Key Words: photocatalysis; flow reaction system; decomposition of NO.

INTRODUCTION

Recently, environmental concerns, namely, the large-scale emission of toxic agents into the atmosphere and water, causing pollution and destruction on a global scale as well as contributing to the greenhouse effect, have made the design of new, clean, and safe chemical processes an urgent issue. NO_x is an especially harmful atmospheric pollutant which causes acid rain, photochemical smog, and the formation of peroxy acetyl nitrates (PAN). The removal of nitrogen oxides (NO_x, $x = 1, 2$), i.e., the direct decomposition of NO_x into N₂ and O₂, has been a great challenge for

many researchers (1–8). The rapid development of surface science and technology has remarkably facilitated progress in understanding the physical and chemical properties of semiconductor materials and, especially, titanium dioxide (TiO₂). As a photocatalyst, titanium dioxide has attracted extensive interest due to its various attractive properties as a low-temperature, nontoxic, highly stable, low-cost, and highly reactive catalyst for chemical waste remediation (8–17). The basic principle of such photocatalysis involves the migration of photogenerated electrons (e⁻) and holes (h⁺) to the surface which serve as redox reactants, leading to surface catalytic reactions.

As one of the most popular photoactive catalysts, TiO₂ photocatalysts have long been investigated in different forms as bulk materials, colloidal suspensions, and dispersed into SiO₂ matrices and on porous supports such as zeolites and porous Vycor glass (2, 4, 6, 7). Although the utilization of extremely small powdered nanosize TiO₂ particles has attracted a great deal of attention due to their high photocatalytic reactivities, the actual factors controlling the photocatalytic activity of the catalyst are still unknown, especially under a large-scale flow system for the photocatalytic decomposition of NO.

Along these lines, in the present paper, we have investigated the photocatalytic decomposition of NO on well-characterized standard reference powdered TiO₂ photocatalysts under a large-scale flow reaction system. Special attention has been focused on the effects of the pretreatment and reaction conditions on the reaction and conversion rates of NO. The present study demonstrates that the photocatalytic decomposition of NO on TiO₂ can be carried out under a large-scale flow system continuously and with high efficiency. Furthermore, the pretreatment and reaction conditions were investigated to achieve the highest efficiency. It was also confirmed that the surface hydroxyl groups play a significant role as active sites for the decomposition of NO.

¹ Permanent address: Institute of Fine Chemicals, East China University of Science and Technology, Shanghai 200237, P. R. China.

² To whom correspondence should be addressed.

EXPERIMENTAL

Photocatalytic flow reaction system. The photocatalytic reaction carried out under a flow system is shown in Fig. 1. The flow rates of the reactant gases (NO, He) and pretreatment gases (Ar, O₂) were adjusted with a mass flow controller. An electronic furnace was used for the pretreatment of the catalysts under an O₂ and Ar flow at suitable temperatures. During the photoreactions, to keep the Hg lamp cool and to absorb the infrared beams emitted, water was circulated in cooling pipes made of quartz glass.

An NO_x meter (New Cosmos Electric Motors, Ltd.) and gas chromatograph were used to measure the NO and product (N₂, O₂, and N₂O) concentrations. The reaction cell was made of quartz (length, 190 mm; inner diameter, 10 mm). A 150 mg portion of the TiO₂ photocatalyst was introduced into the cell. To prevent any movement of the catalyst in the cell, glass wool was placed at both the bottom and top sides of the reaction cell. The NO_x meter and gas chromatograph were connected to continuously measure and record the changes in the concentrations of NO and the products N₂, O₂, and N₂O.

Catalysts. Five different types of ultrafine powdered TiO₂ catalysts (grain size, 0.02–1 μm) supplied by the Catalysis Society of Japan as standard reference TiO₂ (JRC-TIO-2, -3, -4, and -5) were used as the photocatalysts. Detailed information on these catalysts is available from the Catalysis Society of Japan, but is also given in Table 2.

Characterization method. The UV absorption spectra were recorded with a Shimadzu UV-2200A spectrometer at 295 K. The laser-induced Raman spectra were measured with a JASCO NR-1000 Raman spectrometer equipped with an NEC GLS-3200 gas laser.

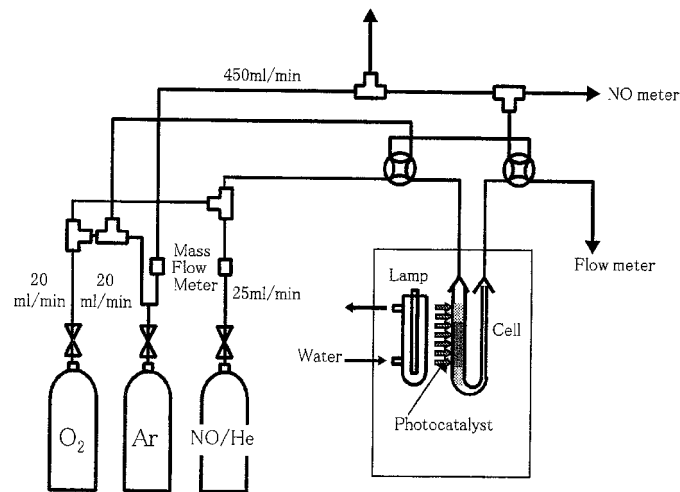


FIG. 1. Flow system for the photocatalytic reaction of NO_x.

Photocatalytic decomposition of NO. The photocatalytic reactions observed under the flow system are shown in Fig. 1. The flow reactant gases and the pretreatment gases were introduced from the bottom side of the catalyst layers. A 150 mg portion of the TiO₂ photocatalyst was loaded in the reaction cell which was then connected to the flow system with silicone grease. The TiO₂ photocatalyst was heated in O₂ using an electronic furnace, and then treated with Ar flow gas at 20 cm³/min. When the temperature of the photocatalyst reached the appropriate temperature, O₂ and Ar flow gases were introduced into the cell for 2 h at 20 cm³/min, respectively. The system was then cooled to the reaction temperature (e.g., 298 K, 373 K, 473 K, 573 K, 673 K, and 723 K), and the O₂ flow was discontinued, while the Ar flow was continued for 1 h more at a flow rate of 20 cm³/min. After these pretreatment procedures were carried out, the reaction cell was cooled to room temperature under an Ar gas flow.

In the photocatalytic reaction, the concentration of the NO reactant gas (mixture of NO and helium) was 10 ppm, and the flow rate of the reactant gas was 100 cm³/min. After reaching a steady state, UV irradiation was started and continued for 2 h. A Toshiba SHL-100UV high-pressure Hg lamp was used. The distance of the lamp from the reaction cell was 10 cm and a color filter of UV-27 (λ > 270 nm) was used. The photon density of the Hg lamp passing through the UV-27 filter was 10,790 lx as measured by a digital lux meter, model LX-1332.

RESULTS AND DISCUSSION

1. Effect of Pretreatment Conditions

The relationship between the photocatalytic reactivity of the TiO₂ photocatalysts and the reaction temperature for the photocatalytic decomposition of NO was studied, and we found the reaction efficiency to be the highest when the photocatalytic reaction was carried out at room temperature (298 K) (18). Other effects, such as that of the pretreatment temperature of the TiO₂ catalyst with O₂ and Ar on the photocatalytic activity, were also investigated. The pretreatment temperature can alter the surface properties of the catalysts, i.e., of the active sites. Figure 2 shows the reaction time profiles of the photocatalytic decomposition of NO at room temperature on the JRC-TIO-4 photocatalyst pretreated with a mixture of O₂ and Ar at 573 K, respectively. In each run, the Ar pretreatment temperatures were also changed from 295 K, 373 K, 473 K, 573 K, 673 K, to 723 K. In the photocatalytic reaction, the concentration of NO was 10 ppm and the reactant gas flow rate was 100 cm³/min. From Fig. 2, it can be seen that the photocatalytic reactivity increased with an increase in the Ar pretreatment temperature and the highest reactivity was found at 573 K.

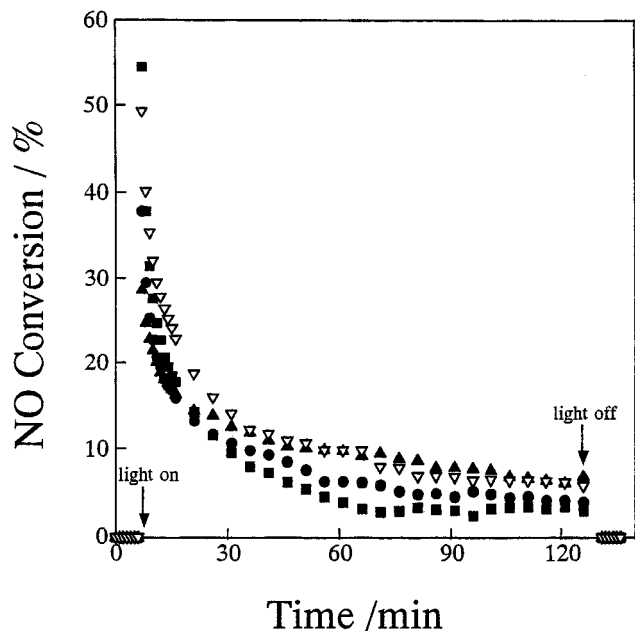


FIG. 2. Reaction time profiles of the photocatalytic decomposition of NO at room temperature on the TiO₂ photocatalyst pretreated with O₂ at 573 K. Pretreatment: under a flow of O₂ (20 cm³/min) and Ar (20 cm³/min) at 573 K, heated in an Ar flow (20 cm³/min) at 295 K (●), 373 K (■), 473 K (▲), and 573 K (▽), respectively. Gas component: 10 ppm NO, 100 cm³/min. Catalyst: JRC-TIO-4, 150 mg.

Figure 3a shows the conversion of NO at different Ar pretreatment temperatures (295 K, 373 K, 473 K, 573 K, and 673 K) when the O₂ pretreatment temperature is constant at 673 K. In this case, at first, the photocatalytic reactivity is enhanced with the increase in Ar pretreatment temperatures from 295 K to 573 K. However, further increases up to 673 K caused a decrease in the photocatalytic reactivity.

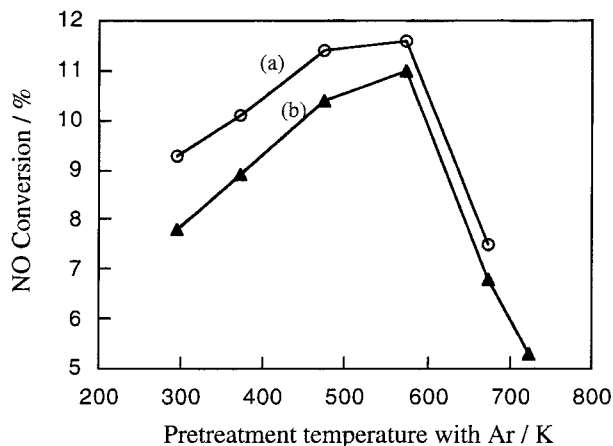


FIG. 3. Effect of the pretreatment of Ar on the conversion of NO at a reaction time of 0.5 h on the JRC-TIO-4 catalyst. Pretreatment of the flow mixture of O₂ (20 cm³/min) and Ar (20 cm³/min) at (a) 673 K (○), and (b) 723 K (▲), respectively. Gas component: 10 ppm NO, 100 cm³/min. Catalyst: JRC-TIO-4, 150 mg.

Figure 3b shows the conversion of NO at different Ar pretreatment temperatures (295 K, 373 K, 473 K, 573 K, 673 K, and 723 K) when the O₂ pretreatment temperature is constant at 723 K. The results are the same as those shown in Fig. 3a and they suggest that an Ar pretreatment temperature of 573 K is the optimum for achieving the highest photocatalytic reactivity.

Figure 2 also shows that these photocatalysts gradually lose their photocatalytic reactivity during photoreactions carried out on a large-scale and for a long period. After 2 h, the conversion of NO for each photocatalyst levels off and becomes one-fourth to one-fifth of the photocatalytic reactivity observed at the beginning of the reaction. Thus, the decline in the photocatalytic reactivity of TiO₂ for the decomposition of NO in the absence of O₂ and/or H₂O could be confirmed. The reaction products of the decomposition of NO under the flow system were also confirmed to be N₂, O₂, and N₂O, as for the closed reaction system.

In order to further investigate the effects of the pretreatment temperature of TiO₂ on the photoreactivity, the Ar pretreatment temperature was fixed at 573 K, while the O₂ and Ar gas mixture pretreatment temperatures were changed from 573 K and 673 K to 723 K. In this case, increasing the pretreatment temperature was found to cause a decline in the photocatalytic reactivity. It was found that a pretreatment temperature of 573 K for O₂ and Ar is the most suitable for achieving a high reactivity for the decomposition of NO in the flow system.

From the above results, it was found that when the pretreatment temperatures are lower than 573 K, the adsorbed water and the organic compounds are adsorbed on the surface of TiO₂, forming active sites for photocatalysis to take place. On such active sites, the reactant NO molecules are able to adsorb and act as precursors for the photocatalytic reaction. It is well known that the local surface structure plays a very important role in the decline of the efficiency in heterogeneous catalysis and photocatalysis since the interaction of the reactant molecules with the surface active sites, i.e., the adsorption process, significantly influences the reaction rate. For the photocatalytic decomposition of NO on TiO₂, the surface hydroxyl groups on the catalysts are known to play a vital role in the reaction (19, 20). When the pretreatment temperature is higher than 573 K, the surface hydroxyl groups are eliminated from the photocatalyst surface as H₂O. Such elimination of the surface OH groups leads to a decline in the photocatalytic activity of the catalyst. These observations have been supported by our present results.

After the photocatalyst was pretreated at 723 K, the FTIR spectra were measured. They clearly showed a sharp peak at around 3720 cm⁻¹ which could be assigned to the "free" -OH stretching vibration. When the TiO₂ photocatalyst was pretreated at 573 K, there were two types of surface -OH bands around 3660 cm⁻¹ and 3680 cm⁻¹, besides the peak around 3720 cm⁻¹. The bands around

3660 cm^{-1} and 3680 cm^{-1} are considered to be hydroxyl groups which react with each other through hydrogen bonding. An increase in the pretreatment temperature led to a decrease in surface hydroxyl groups having hydrogen bonds (18). Therefore, after pretreatment of TiO_2 at high temperatures, the hydroxyl groups on the surface acted as free OH groups and these species become the active sites for the decomposition of NO under the flow system.

Figure 2 also shows that the conversion rates of NO are very high at the beginning of the reaction; however, with prolonged reaction time, a decline in the photocatalytic reactivity takes place. After UV irradiation for 2 h, the rate of the conversion of NO achieved a steady state and a showed constant rate. It can be considered that at the beginning of the reaction, the conversion of NO involves the decomposition of NO as well as the adsorption of NO on the surface of the TiO_2 photocatalyst.

2. Surface Properties of the TiO_2 Photocatalysts

The UV-vis absorption spectra of five different types of powdered standard reference TiO_2 catalysts are shown in Fig. 4. The bandgap energies of these catalysts differ with their crystalline structures; i.e., rutile is located at 410 nm and anatase at 390 nm. Figure 4 shows that the UV absorption bandgap positions of JRC-TIO-3 and -5, which have

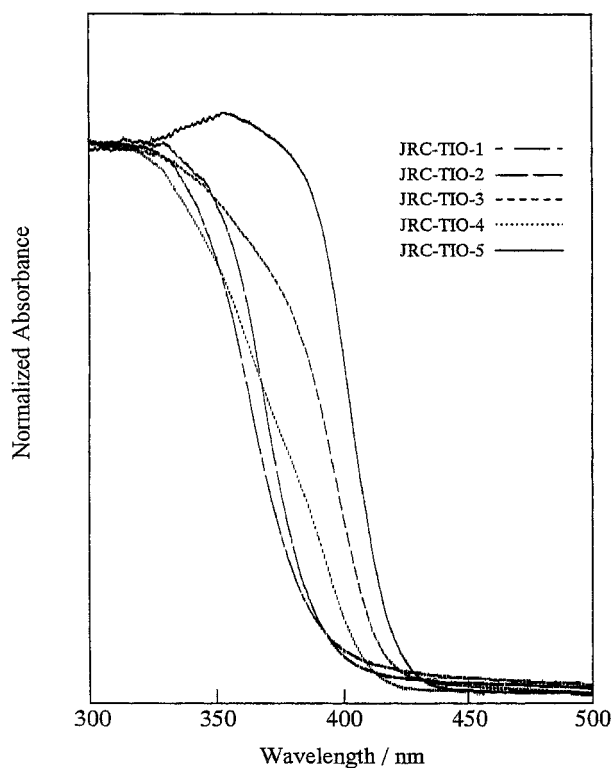


FIG. 4. UV-vis diffuse reflectance absorption spectra of the standard TiO_2 reference photocatalysts.

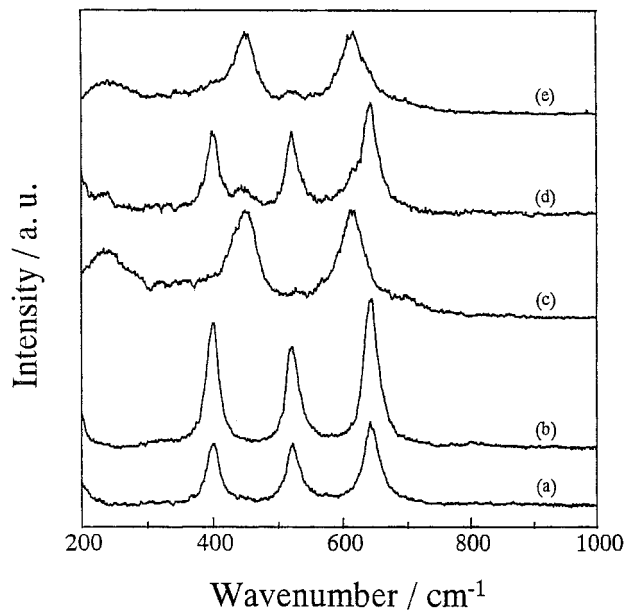


FIG. 5. Raman spectra of the standard TiO_2 reference photocatalysts: (a) JRC-TIO-1, (b) JRC-TIO-2, (c) JRC-TIO-3, (d) JRC-TIO-4, and (e) JRC-TIO-5. All spectra were obtained in ambient air.

rutile structures, can be found around 410 nm, while the UV absorption bandgap position of JRC-TIO-1 and -2, which are anatase, can be found around 390 nm. From Fig. 4, it can be seen that the JRC-TIO-4 catalyst is mainly anatase with small amounts of rutile.

The results of the laser Raman spectra are shown in Fig. 5. According to reports by Damen and Gilson (21, 22), the peaks around 144 cm^{-1} (b_{1g}), 488 cm^{-1} (e_g), 611 cm^{-1} (a_{1g}), and 828 cm^{-1} (b_{2g}) are assigned to the rutile structures while the peaks around 144 cm^{-1} (e_g), 197 cm^{-1} (e_g), 400 cm^{-1} (b_{1g}), 515 cm^{-1} (b_{1g}), 519 cm^{-1} (a_{1g}), and 640 cm^{-1} (e_g) can be assigned to anatase. In Fig. 5, peaks around 448 cm^{-1} and 616 cm^{-1} which are assigned to rutile can be observed with JRC-TIO-3 and -5, while peaks around 400 cm^{-1} , 524 cm^{-1} , and 644 cm^{-1} , which are assigned to anatase, can be observed with JRC-TIO-1, -2 and -4. However, the peak around 445 cm^{-1} , having a rutile structure, can also be observed with JRC-TIO-4. It can be deduced from these results that the JRC-TIO-4 catalyst contains both anatase and rutile, and these laser Raman spectra results are in good agreement with the UV absorption spectra.

3. Photocatalytic Decomposition of NO in the Flow System

UV irradiation of the reference standard TiO_2 catalysts in the presence of NO led to the decomposition of NO into N_2 , O_2 , and N_2O under a flow system. Figure 6 shows the conversion of NO on these different types of catalysts under UV irradiation with the irradiation time. The pretreatments of the catalysts were all carried out at 573 K.

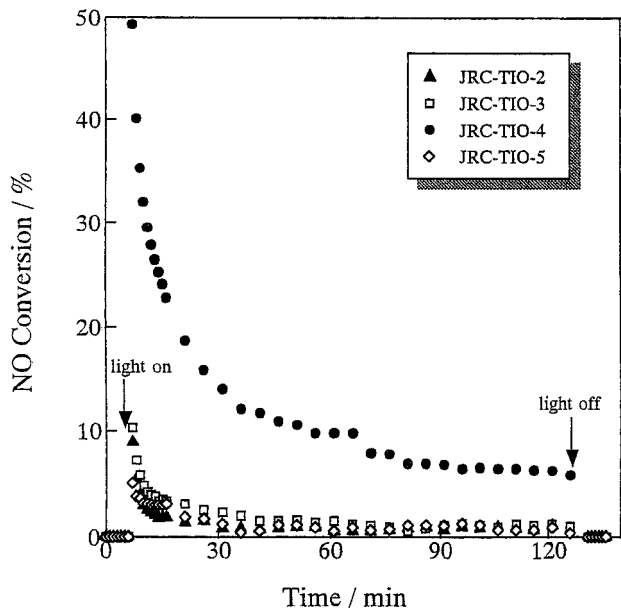


FIG. 6. Reaction time profiles of the photocatalytic decomposition of NO on the standard TiO₂ reference photocatalyst at room temperature. Pretreatment: under a flow of O₂ (20 cm³/min) and Ar (20 cm³/min) at 573 K, heated in an Ar flow (20 cm³/min) at 573 K. Gas component: 10 ppm NO, 100 cm³/min. Catalyst: 150 mg.

Figure 7 shows the conversion of the photocatalytic decomposition of NO at room temperature. JRC-TIO-4 shows the highest photocatalytic activity of all the reference catalysts. However, apart from JRC-TIO-4, the photocatalytic activity of the other catalysts scarcely differed, as can also be seen in Fig. 7. The photoactivities measured by the conversion of NO were in the following order: JRC-TIO-4 > -3 >

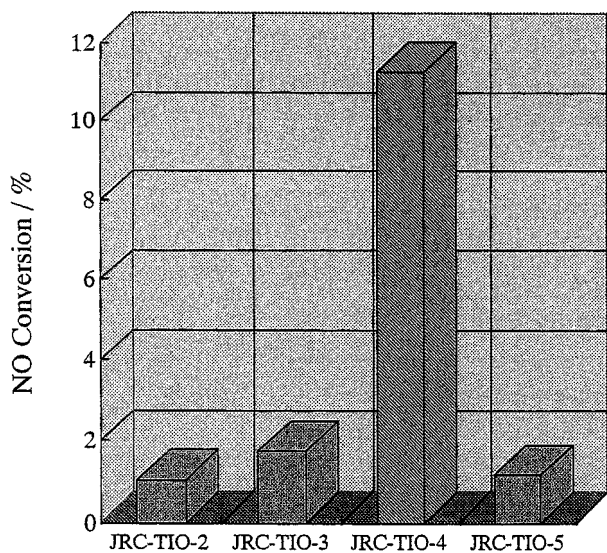


FIG. 7. Conversion of the photocatalytic decomposition of NO on the standard reference TiO₂ photocatalysts at room temperature.

TABLE 1

Photocatalytic Reactivities of the Standard Reference TiO₂ Photocatalysts for Different Types of Reactions

Catalyst (JRC-TIO-)	Reduction of CO ₂ (μmol/h · g)	Hydrogenation of methyl acetylene (μmol/h · g)	Isomerization of <i>cis</i> -2-butene (μmol/h · g)
2 (anatase)	0.03	0.20	2.5
3 (rutile)	0.02	0.12	1.0
4 (anatase)	0.17	8.33	9.4
5 (rutile)	0.04	0.45	3.8

-5 > -2. These results are slightly different from those of the reactions investigated for the hydrogenolysis of methyl acetylene with H₂O, the isomerization of 2-butene, the reduction of CO₂ with H₂O, and ethylene oxidation with O₂ in the presence of H₂O (19, 20). The photocatalytic activities of the standard reference TiO₂ photocatalysts in these reactions are shown in Table 1. The difference in reaction systems (i.e., a flow system or a hermetic system) may have caused the variances in the order of their photoactivities. In this case, the photocatalytic reactivity was determined by the conversion of NO; however, in the other cases (Table 1), it was determined by the yields of the photoformed products.

The typical chemical/physical properties of these standard reference TiO₂ catalysts are shown in Table 2. The relative surface -OH concentration was calculated from the intensities of the IR peak assigned to the surface OH group on TiO₂. The concentration of the surface acidic sites was calculated from the peak intensities of the observed temperature-programmed desorption (TPD) patterns of the preadsorbed NH₃ on TiO₂. From Fig. 7 and Table 2, it can be seen that the anatase TiO₂ catalysts with large surface areas, large bandgaps, and numerous surface -OH groups exhibit highly efficient photocatalytic reactivity for the decomposition of NO, indicating that these are the main conditions prerequisite to achieve high photocatalytic reactivity. The increased bandgap is accompanied by a shift in the conduction band edge to higher negative energies, moving the reductive potential to more negative values and

TABLE 2

Physicochemical Properties of the Standard Reference TiO₂ Photocatalysts

Catalysts (JRC-TIO-)	Surface area (m ² /g)	Acid concn (μmol/g)	Relative -OH concn	Band gap (eV)
2 (anatase)	16	6	1	3.47
3 (rutile)	51	22	1.6	3.32
4 (anatase)	49	5	3.0	3.50
5 (rutile)	3	7	3.1	3.09

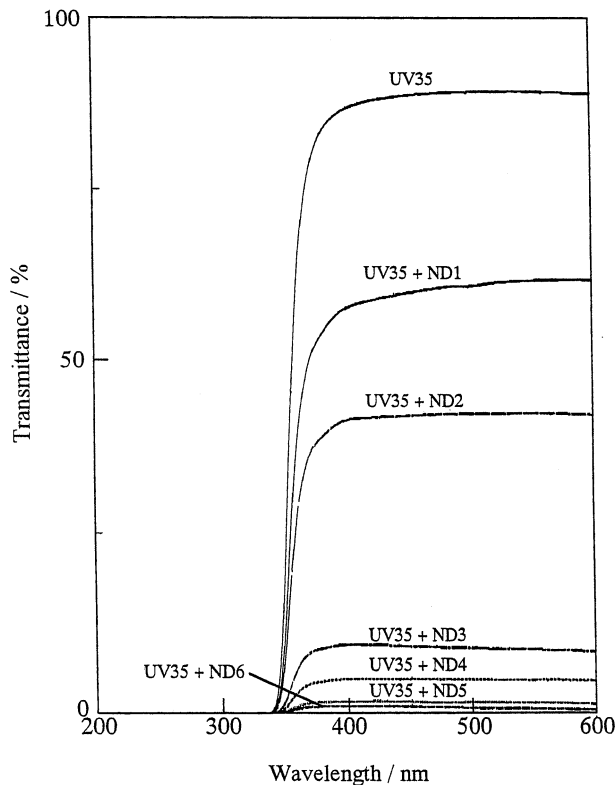


FIG. 8. Characteristics of the UV-vis transmittance of the various UV cut filters.

thus enhancing the photocatalytic reactivity. It is also suggested that the surface $-OH$ groups and/or the physisorbed H_2O play a significant role in the photocatalytic reactions through the facile formation of reactive OH radicals (18).

The intensity of the incident light is also a very important factor in determining the rate of the photocatalytic decomposition reaction of NO . In order to investigate the effects of the incident light intensity on the rate of the photocatalytic reaction, the photocatalytic efficiency was monitored by changing the relative intensity of the incident light from 250 lx to 16,750 lx by using ND filters, as shown in Fig. 8. According to the UV-vis absorption measurements, the intensity of the light passing through a UV-35 filter alone was 100% (16,750 lx) while their relative light passing intensities were 70% (11,860 lx), 47% (8070 lx), 10% (2050 lx), 5% (1150 lx), 2% (410 lx), and 1% (250 lx) when the UV-35 filter was used with ND1, ND2, ND3, ND4, ND5, and ND6, respectively.

Figure 9 shows the effect of the intensity of the incident light on the rate of the photocatalytic decomposition of NO . As can be seen in Fig. 9, the rate decreases with a decrease in the intensity of the incident UV light. Moreover, it can be seen that the reaction efficiency is high at the beginning of the reaction, and then gradually decreases with the reaction time. Such phenomena are the same as those men-

tioned above. In the inset within Fig. 9, we can see that when the intensities of the incident UV light are higher than half of the total intensity, the photocatalytic reaction rates for the decomposition of NO scarcely change. Thus, the photocatalytic reaction rate does not display a linear relationship with the intensity of the incident UV light when its intensity is in relatively strong regions. That is, in the case of such stronger incident beams, the quantum efficiency of the photocatalytic reaction becomes higher when the intensity of the incident beams becomes weaker.

4. Effects of the Addition of O_2 on the Conversion of NO

(1) *Effect of the flow rate of O_2 .* In order to investigate the effects of the flow rates of O_2 on the photocatalytic decomposition of NO , they were varied from 5 cm^3/min and 10 cm^3/min to 20 cm^3/min with a constant 10 ppm NO mixture gas flow rate at 100 cm^3/min , as shown in Fig. 10. As can be seen in Fig. 10, at an O_2 flow rate of 20 cm^3/min , NO and O_2 were mixed in the system and then came in contact with the TiO_2 photocatalyst in the reaction cell. NO was completely removed from the system within 10 min even without UV irradiation due to the adsorption of NO on the photocatalyst and the oxidation of NO with O_2 into NO_2 . Thus, in the presence of O_2 , NO molecules can be easily removed by adsorption and oxidation, but not by a

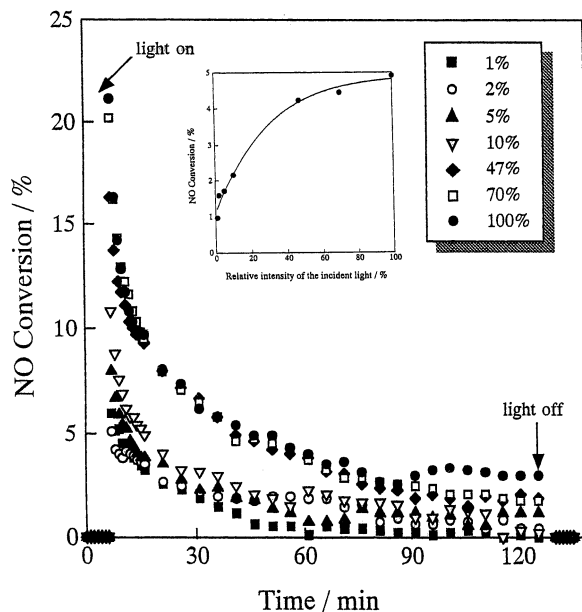


FIG. 9. Effect of the intensity of the incident light on the conversion of NO in the photocatalytic decomposition of NO on the TiO_2 photocatalyst. Relative intensity of the incident light: 1% (\blacksquare), 2% (\circ), 5% (\blacktriangle), 10% (∇), 47% (\blacklozenge), 70% (\square), 100% (\bullet). Pretreatment: under a flow of O_2 (20 cm^3/min) and Ar (20 cm^3/min) at 573 K, heated in an Ar flow (20 cm^3/min) at 573 K. Gas component: 10 ppm NO , 100 cm^3/min . Catalyst: JRC-TIO-4, 150 mg. Inset: Effect of the relative intensity of the incident light on the conversion of NO in the photocatalytic decomposition of NO .

decomposition reaction. The efficiency of such an elimination of NO under dark conditions increased with an increase in the pressure of O₂ in the system.

(2) *Effect of the Mixture of NO and O₂ Gases on the Photocatalytic Decomposition of NO.* There are three different methods for introducing NO and O₂ gas into the flow reaction system, as follows:

- NO gas flow, 30 min → NO/O₂ mixture gas flow, 1 h → irradiation
- O₂ flow, 30 min → NO/O₂ mixture gas flow, 1 h → irradiation
- NO and O₂ mixture gas flow, 1.5 h → irradiation

Before UV light irradiation, the NO and O₂ reactant gases come in contact with TiO₂ for 1.5 h in each introduction process, as shown in Fig. 11. Introduction process (a) reveals the highest conversion of NO as compared with other methods. It is known that the adsorbability of O₂ on TiO₂ is much stronger than that of NO molecules due to its high electron affinity and/or lower electron negativity. If O₂ is introduced into the system, it is easily adsorbed on the surface of TiO₂, and then works to inhibit the adsorption of the NO molecules. In methods (b) and (c), therefore, most of the active sites on the TiO₂ catalysts are occupied by O₂ molecules, resulting in the lower conversion rate of NO molecules than with method (a).

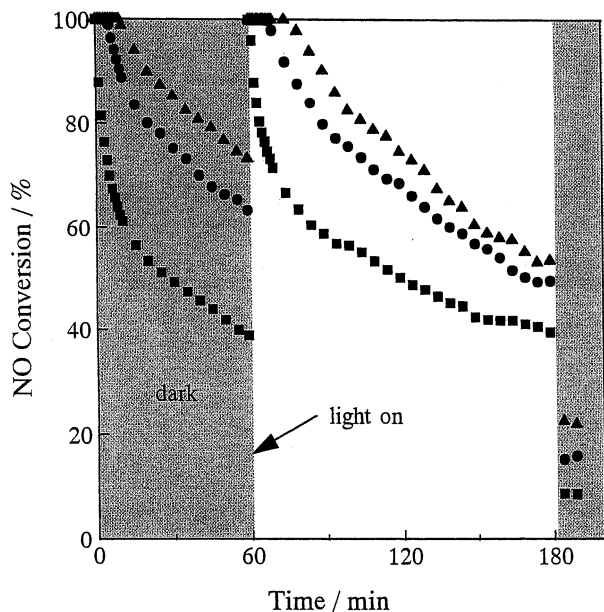


FIG. 10. Reaction time profiles of the photocatalytic decomposition of NO in the presence of O₂ on the TiO₂ photocatalyst at room temperature. O₂ flow rate: (■) 5 cm³/min, (●) 10 cm³/min, (▲) 20 cm³/min. Pretreatment: under a flow of O₂ (20 cm³/min) and Ar (20 cm³/min) at 573 K, heated in an Ar flow (20 cm³/min) at 573 K. Gas component: 10 ppm NO, 100 cm³/min. Catalyst: JRC-TIO-4, 150 mg.

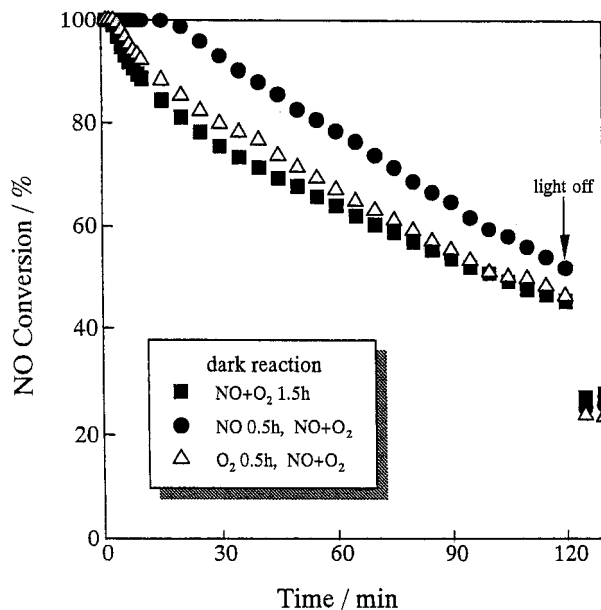


FIG. 11. Reaction time profiles of the photocatalytic decomposition of NO in the presence of O₂ on the TiO₂ photocatalyst at room temperature. Pretreatment: under a flow of O₂ (20 cm³/min) and Ar (20 cm³/min) at 573 K, heated in an Ar flow (20 cm³/min) at 573 K. Gas component: 10 ppm NO, 100 cm³/min. Catalyst: JRC-TIO-4, 150 mg.

CONCLUSIONS

The present study demonstrates that the photocatalytic decomposition of NO on TiO₂ can be carried out under a large-scale flow system for a continuous operation with a high efficiency. The pretreatment and reaction conditions were investigated to achieve the highest efficiency possible. The results showed that pretreatment of the catalyst with a mixture of O₂ and Ar gas at 573 K presents the most optimal conditions for the decomposition of NO under this flow reaction system. Moreover, it was confirmed that the surface hydroxyl groups play a significant role as active sites for the decomposition of NO. The crystalline structures of the standard reference TiO₂ photocatalysts used were well characterized by means of UV absorption and laser Raman spectra measurements. It was found that the conversion rate of the photocatalytic decomposition of NO did not exhibit a linear relationship with the intensity of the incident UV light when the intensity of the incident light was relatively strong. As a result, the quantum efficiency of the photocatalytic reaction was higher with lower intensities of incident light, and lower with higher intensities of incident UV light. The efficiency of the conversion of NO increased with an increase in the O₂ flow rate.

ACKNOWLEDGMENTS

The present work has been supported in part by the "Monbusho Grant-in-Aid for JSPS Fellows" (98096).

REFERENCES

1. Anpo, M., and Yamashita, H., in "Surface Photochemistry" (M. Anpo, Ed.), p. 117. Wiley, Chichester, U.K., 1996.
2. Anpo, M., *Catal. Surv. Jpn.* **1**, 169 (1997).
3. Hoffmann, M. R., Martin, S. T., Choi, W., and Bahnemann, D. W., *Chem. Rev.* **95**, 69 (1995).
4. Fox, M. A., and Dulay, M. T., *Chem. Rev.* **93**, 341 (1993).
5. Ollis, D. F., and Al-Ekabi, H., Eds., "Photocatalytic Purification and Treatment of Water and Air." Elsevier, Amsterdam, 1993.
6. Ichihashi, Y., Yamashita, H., and Anpo, M., *Stud. Surf. Sci. Catal.* **105**, 1609 (1997).
7. Anpo, M., Ichihashi, Y., Takeuchi, M., and Yamashita, H., *Res. Chem. Intermed.* **24**(2), 143 (1998).
8. Serpone, N., and Pelizzetti, E., "Photocatalysis." Wiley, New York, 1989.
9. Fan, J., and Yates, J. T., Jr., *J. Am. Chem. Soc.* **118**, 4686 (1996).
10. Lichtin, N. N., and Avudaithai, M., *Environ. Sci. Technol.* **30**, 2014 (1996).
11. Yamashita, H., Zhang, S. G., Matsumura, Y., Souma, Y., Tatsumi, T., and Anpo, M., *Appl. Surf. Sci.* **121&122**, 305 (1997).
12. Alekabi, H., and Serpone, N., *J. Phys. Chem.* **92**, 5726 (1988).
13. Yamashita, H., Honda, M., Harada, M., Ichihashi, Y., Anpo, M., Hirao, T., Itoh, N., and Iwamoto, N., *J. Phys. Chem. B* **102**, 10707 (1998).
14. Yamashita, H., Kawasaki, S., Ichihashi, Y., Harada, M., Takeuchi, M., Anpo, M., Stewart, G., Fox, M. A., Louis, C., and Che, M., *J. Phys. Chem. B* **102**, 5870 (1998).
15. Nimlos, M. R., Jacoby, W. A., Blake, D. M., and Milne, T. A., *Environ. Sci. Technol.* **27**, 732 (1993).
16. Grela, M. A., and Colussi, A. J., *J. Phys. Chem.* **100**, 10150 (1996).
17. Anpo, M., Zhang, S. G., Mishima, H., Matsuoka, M., and Yamashita, H., *Catal. Today* **39**, 159 (1997).
18. Kinugawa, K. (M. Anpo, Supervisor), Master Treatise, Department of Applied Chemistry, Osaka Prefecture University, 1996.
19. Park, D.-R., Zhang, J.-L., Ikeue, K., Yamashita, H., and Anpo, M., *J. Catal.* **185**, 114 (1999).
20. Yamashita, H., Ichihashi, Y., Harada, M., Stewart, G., Fox, M. A., and Anpo, M., *J. Catal.* **158**, 97 (1996).
21. Porto, S. P. S., Flourey, P. A., and Damen, T. C., *Phys. Rev.* **154**, 522 (1967).
22. Beattie, I. R., and Gilson, T. R., *Proc. R. Soc. London, A* **307**, 407 (1968).